# NEW DEVELOPMENTS IN LOW-Z GAS STRIPPER SYSTEM AT RIKEN RADIOACTIVE ISOTOPE BEAM FACTORY (RIBF)

H. Okuno*, N. Fukunishi, A. Goto, H. Hasebe, H. Imao, O. Kamigaito, M. Kase, H. Kuboki
RIKEN, Nishina Center for Accelerator-Based Science, Hirosawa, Wako 351-0198, Japan

*Abstract*

The RIKEN radioisotope beam factory (RIBF) has been successfully operated for more than five years as the first next-generation exotic beam facility after the extraction of the first beam at the end of 2006. Continual development efforts in these five years have led to improved performance of the accelerators, thereby leading to increase in the intensity of the various heavy-ion beams that have been produced. Furthermore, the operation of a new 28-GHz superconducting electron cyclotron resonance (ECR) ion source and a new injector linac was started from October 2011 to overcome the difficulty in increasing the uranium beam intensity that is currently far below our goal of 1 pμA ($6 \times 10^{12}$ particles/s). However, the most serious problem, which is the design and implementation of a charge stripper for high-power uranium beams, has thus far remained unsolved, despite extensive R&D studies on strippers using large foils mounted on a rotating cylinder and the study of a $N_2$ gas stripper. A gas stripper is free from problems related to lifetime issues and uniformity in stripper thickness, although the equilibrium charge state in such a stripper is considerably lower than that in a carbon foil stripper owing to the absence of the density effect. These merits of gas strippers have motivated us to develop a low-Z gas stripper to achieve a higher equilibrium charge state even in gases, by virtue of suppression of the electron capture process in low-Z gas. In this light, we carried out the following R&D programs. The first one included the measurement of the electron-loss and electron-capture cross sections of uranium ions in He gas to extract the equilibrium charge state. The second study obtained measurements of charge distributions and energy spreads using thick layers of windowless He gas targets. The results of these studies were satisfactory, and it was decided to practically construct the proposed machine for He gas stripping. We constructed and installed the new He gas stripper for the operation of an uranium beam in January 2012. Tests using uranium beams are in progress before the the uranium beam series, which is scheduled for the coming autumn 2012.

## INTRODUCTION

### *RI Beam Factory*

The RIKEN Nishina Center for Accelerator-Based Science constructed the RadioIsotope Beam Factory (RIBF) [1] with the aim of realizing a next-generation facility that can produce the most intense RI beams in the world at energies of several hundred mega-electronvolts per nucleon over the entire range of atomic masses. The RIBF facility includes an accelerator complex that can accelerate ions over the entire range of masses and deliver 80-kW uranium beams at an energy of 345 MeV/u. Figure 1 shows a bird's eye view of the RIBF. The section on the left indicates the old facility that was completed in 1990. Many experiments have been carried out with light-ion RI beams using the four-sector K540-MeV RIKEN ring cyclotron (RRC) with two injectors, the RIKEN linear accelerator (RILAC), and the AVF cyclotron. The feasibility of conducting such light-ion experiments is enabled by the fact that the RRC can accelerate relatively light ions up to 100 MeV/u, which is the value of the lower limit for RI beam production. In order to expand the mass range for RI beam production up to that of uranium, three ring cyclotrons, the fixed-frequency ring cyclotron (fRC), the intermediate-stage ring cyclotron (IRC), and the superconducting ring cyclotron (SRC) were designed and constructed as energy boosters for the RRC.

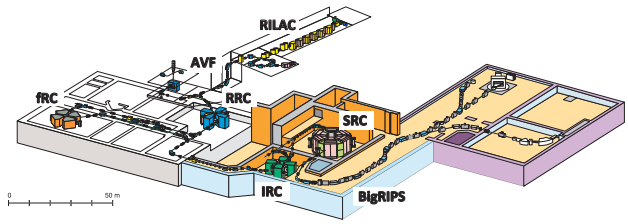


Figure 1: Bird's eye view of RI Beam Factory.

The design and construction of the RIBF accelerators was begun in 1997, and the accelerator building was completed at the end of March 2003. In November 2005, an important milestone was reached; the superconducting sector magnets for the SRC were successfully excited at the maximum field level. The first beam was obtained on December 28, 2006 [2]. Many improvements have since been carried out to increase the beam intensity and to commission new beam species to meet the requirements of different experiments. Furthermore, the operation of the new injection system that consists of a 28-GHz superconducting ECR ion source (SC-ECRIS) [3] and a linac (RILAC2) [4] was started in October 2011 to overcome the difficulty in increasing the uranium beam intensity, whose current value is far below our goal of 1 pμA ($6 \times 10^{12}$ particles/s) [5]. The SC-ECRIS was designed to have a large plasma vol-

* okuno@riken.jp

ume of 1100 $cm^3$ and to provide a flat magnetic field distribution in the central region by exciting the corresponding solenoid independently [6]. The RILAC2 is designed to efficiently accelerate ions with a mass-to-charge ratio of 7, thus aiming at the production of heavy ions such as $^{84}Kr^{13+}$, $^{136}Xe^{20+}$, and $^{238}U^{35+}$, up to an energy of 670 keV/nucleon. It mainly consists of an RFQ linac based on the four-rod structure and three drift-tube linacs (DTLs) based on a quarter-wavelength resonator (QWR).

Table 1 lists the beams accelerated at maximum intensity thus far. These beams have been used in many nuclear experiments including that of the discovery of 45 new isotopes [7], the study of the halo structure and large deformation of extremely neutron-rich Ne isotopes [8, 9] and measurements of the $\beta$-decay half-lives of very neutron-rich Kr to Tc isotopes on the boundary of the r-process path, thereby indicating fast r-matter flow [10]. Our goal is to achieve a beam intensity of 1 pμA for the entire atomic range. This target intensity has been achieved for He and O. The beam intensity of Ca is 415 pnA which is the current world record. The beam intensities of very heavy ions such as Xe and U ion are still relatively small; however, these intensities are increasing due to the operation of the new injector system from October 2011. Further developments in SC-ECRIS are expected to increase the U and Xe beam intensities up to 100 pnA in the next few years, which clearly indicates that the problems with respect to the charge strippers for uranium acceleration will be more severe.

Table 1: List of beams accelerated at RIBF accelerator complex along with corresponding maximum beam intensity achieved.

| **Ion** | **Energy** (MeV/u) | **Intensity** (pnA) | **Date** |
|---|---|---|---|
| polarized $^2H$ | 250 | 120 | May 2009 |
| $^4He$ | 320 | 1000 | Oct 2009 |
| $^{14}N$ | 250 | 80 | May 2009 |
| $^{18}O$ | 345 | 1000 | Jun 2010 |
| $^{48}Ca$ | 345 | 415 | May 2012 |
| $^{70}Zn$ | 345 | 100 | Jul 2012 |
| $^{86}Kr$ | 345 | 30 | Nov 2007 |
| $^{124}Xe$ | 345 | 27 | Jun 2012 |
| $^{238}U$ | 345 | 3.5 | Dec 2012 |

## *Charge Strippers for Uranium Acceleration in FAIR, RIBF, and RIBF*

Charge strippers in an accelerator complex play an essential role in breeding the required state of a given ion. The charge state $Q$ is related to the in the equation of motion of the ion as below:

$$\frac{d\boldsymbol{v}}{dt} = \frac{Q}{M}(\boldsymbol{E} + \boldsymbol{v} \times \boldsymbol{B}) \quad (1)$$

Here, $\boldsymbol{v}$, $M$, $\boldsymbol{E}$ and $\boldsymbol{B}$ denote the ion velocity, ion mass, electric field and magnetic field, respectively. Therefore $Q$ is the sensitivity to $E$ and $B$, which contribute to beam acceleration, bending, or focusing. The charge state of the ion is a function of projectile energy (Fig. 2) after being passed through a sufficiently thick stripper to reach a state of equilibrium in where electron loss and capture are balanced.

The general requirements of charge strippers are as follows. Firstly, a high charge state is preferred in order to reduce the total accelerating voltage and cost. In this sense solid or liquid strippers are desirable because the density effect in these states can provide approximately 20% higher charge states compared to that for gas. Secondly, the stripping efficiency should be as high as possible although the typical efficiency is around 20%. It is to be noted at this stage that using a large number strippers can decrease the beam intensity to zero. Thirdly, a stripper should possess longevity and operational durability. In particular lifetime-related problems are critical to high-power beam operation because the lifetime of the stripper is anti-proportional to the irradiated beam intensity. Finally the thickness of the stripper should be uniform. Non-uniformity in stripper thickness generates additional energy spread or emittance growth in the longitudinal direction, and this can cause undesirable beam loss in the succeeding accelerators stages.

Table 2 lists the shows specifications of the charge strippers required for the three primary uranium accelerators installed in FAIR, FRIB, and RIBF along with their technical implementation challenges. The accelerator in FAIR accelerates uranium ions up to 1500 MeV/u using synchrotrons. One stripper is installed at the 1.4 MeV/u ion energy stage to increase ion charge from 4+ to 28+ as shown in Fig. 2. The peak power of the pulsed beam is about 1.5 MW at this stripper. The charges are stripped by $N_2$ gas introduced by a supersonic gas jet. The acceleration of intermediate charge state ions such as $U^{28+}$ ions is very essential to reduce the effect of space charge forces. This reduction allows for higher beam intensities. Furthermore the accelerator at FAIR is free from any problems with respect to charge stripping of ions with energies of around 10 MeV/u; in general, charge stripping is potentially problematic in this energy region. However, the FAIR accelerator faces the technical challenge of dynamic vacuum. Intermediate charge state heavy ions such $U^{28+}$ ions are exposed to a high probability of charge exchange due to collisions with residual gas molecules during their acceleration. Since the charge exchange process changes the ions' magnetic rigidity, the involved ions are lost behind dispersive elements, and an energy-dependent gas desorption takes place. The desorbed gas is another source of the charge exchange. The FRIB accelerates uranium ions up to energies of 200 MeV/u using SRF linacs. One stripper is installed at the 16.3 MeV/u ion energy stage to increase charge from 33.5+ to 78+ on average as shown in Fig. 2. Nearly 80% of the input ions can be gathered at the output using the multi-charge acceleration technique [11]. The average beam power at the stripper is about 40 kW. A liquid

Table 2: Charge stripper specifications for uranium acceleration at FAIR, FRIB, and RIBF. The term PW in the table denotes 'plasma window'.

| Item | FAIR | FRIB | RIBF |
|---|---|---|---|
| Final energy | 1.5 GeV/nucleon | 200 MeV/u | 345 MeV/u |
| Type of accelerator | Synchrotron | SRF linac | Cyclotron |
| Number of charge strippers | 1 | 1 | 2 |
| Stripping energy | 1.4 MeV/u | 16.3 MeV/u | 11 and 51 MeV/u |
| Charge state | 4→28 | 33, 34→76-80 | 35→(71/65)→86 |
| Stripping efficiency | ~14% | ~80% | ~5% |
| Beam power at stripper | 1.5 MW (pulsed) | 40 kW | 7.5 kW |
| Type of stripper | $N_2$ gas (supersonic gas jet) | Liq. Li film (baseline) He gas with PW (alternative) | C-foil → He gas (1st stripper) C-foil (2nd stripper) |
| Technical challenge | Dynamic vacuum | Liq. Li film and PW | He gas confinement |

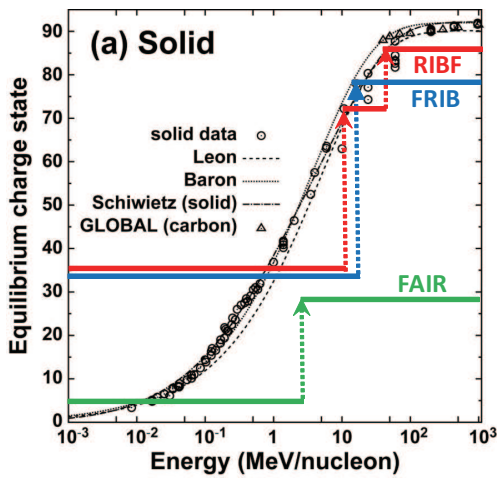


Figure 2: Charge evolutions in uranium acceleration for FAIR, FRIB and RIBF as a function of projectile energy with equilibrium charge state.

lithium film [12] has been adopted as baseline choice of stripper. In order to make liquid lithium film, a rounded lithium jet from a nozzle is impacted on the edge of the deflector. The stability of the film has been successfully demonstrated under actual operating conditions. The alternative stripper available for use is the He gas stripper [13] sandwiched between two plasma windows [14]. The plasma window can reduce conduction by a factor of about 20, thereby leading to improved He gas confinement. The operation of the system has been successfully demonstrated with a window aperture of 2 mm. Scientists at the FRIB facility are attempting to increase beam aperture from 2 mm to more than 6 mm. The RIBF accelerates uranium ions up to 345 MeV/u via the use of cyclotrons. Two charge strippers are installed to increase charge from 35+ to 86+ as shown in Fig. 2. The stripping efficiency is extremely low because of the adoption of the two-step stripping approach. In the rest of the paper, we examine the charge strippers for use in the RIBF.

## CHARGE STRIPPER PROBLEM FOR URANIUM ACCELERATION AT RIBF

Figure 3 shows the RIBF acceleration scheme for uranium beams with the use of two strippers. Uranium beams from the new injector system are accelerated using four cyclotrons, namely, RRC, fRC, IRC, and SRC, up to energies of 345 MeV/u. The first stripper is located behind the RRC, at the ion energy stage of 11 MeV/u, and the second one is located behind the fRC, at the ion energy stage of 51 MeV/u. Carbon foils are used as strippers in both cases. The typical thicknesses of the foils for the first and second strippers are 300 μg/cm$^2$ and 17 mg/cm$^2$, respectively. The problem associated with the first stripper is extremely grave from the viewpoint of our operational experiences. Carbon foils commercially available are currently being used for the first stripper. The carbon foils clearly show radiation damage, and the momentum spread of the beam after it passes through the stripper becomes wider after beam irradiation. Their typical lifetime is about 12 h at intensities of 1-2 eμA. Carbon foils of identical thicknesses are being developed at RIKEN, and the quality of these foils which is approaching that of the commercially available ones [15]. Table 3 lists the requirements of the first stripper with the performances of the carbon foils. As per beam acceleration requirements, firstly, the charge state at this stripper stage should be more than 69+, which is the lowest acceptable charge state with respect to the succeeding cyclotron fRC. Secondly, from our operational experiences, we hope that a stripper's lifetime should be more than one week at a beam intensity of 100 eμA. Thirdly, the level of non-uniformity in the stripper thickness should be less than 10%. The performance of the carbon foils (listed in Table 3), clearly shows that a stripper with a considerably longer lifetime is required for consistent accelerator operation. Therefore, R&D programs focusing on the up-gradation of the first stripper were initiated from 2008.

First, we began conducting irradiation tests on a stripper consisting of a large foil put on a rotating cylinder, which was developed by Ryuto et al. [16], in order to expand the

Table 3: Summary of R&D studies on first charge stripper for uranium acceleration in RIBF

| Item | Value | C-foil | Rotating C-foil | $N_2$ gas | He gas |
|---|---|---|---|---|---|
| Charge | ≥69 | 71 | 71 | 56 | 65 |
| Lifetime | ≥1 week (at 100 eμA) | 12 h (at 1-2 eμA) | 3-4 days (at 10 eμA) | long | long |
| Non-uniformity in thickness | < 10% | ~30% | >30% | 0 | 0 |

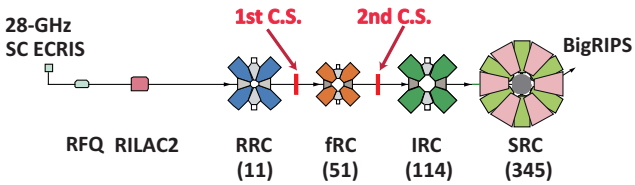


Figure 3: Acceleration scheme for uranium beams using two strippers.

irradiation area, with the objective of realizing long lifetimes. We placed a foil with a diameter of 100 mm on the cylinder, which could be rotated in beam vacuum. The first sample tested in 2008 malfunctioned within a short interval about 15 min. We performed some tests to determine why the rotating foil was prematurely damaged. We found that very slowly (0.05 rpm) rotating carbon nanotube (CNT)-based foils can survive for three or four days at intensities of 10 eμA. Some foil sections were missing after three or four days and the foil required replacement. However, despite the above-mentioned issues, this stripping system was successfully used in the uranium beam series the last year when the RILAC2 became operational as an injector.

Next, we initiated the development of gas strippers. A gas stripper is free from lifetime-related problems although it provides a lower equilibrium charge state than a carbon foil due to absence of the density effect. We did not have data on the equilibrium charge state in $N_2$ gas, and no empirical formulae are currently available to predict the equilibrium charge state correctly. Therefore, we measured the charge state at 11 MeV/u using a gas target system with a differential pumping system that was formerly used for nuclear experiments [17]. The measured equilibrium charge state in $N_2$ was 56+, which is far below that in a carbon foil (71+), thereby suggesting that the gas stripper cannot be used for uranium because the acceptable charge state for the fRC is larger than 69+.

Details of the two R&D studies on the charge stripper are summarized in Table 3. The lifetime of the rotating foil is not sufficiently long because we expect an increase in the beam intensity in future beam accelerations. The beam quality after the beam passes through the stripper is quite poor, thereby suggesting that the non-uniformity in the stripper thickness is larger than 30%. In contrast, the lifetime of the gas stripper is sufficiently large, and its uniformity in therms of thickness is good, although the equilibrium charge state is so low that fRC cannot accept the U ions. Therefore, the merits of using a gas stripper motivated us to develop a low-Z gas stripper that may provide higher charge states even in gas.

## R&D STUDIES ON LOW-Z GAS STRIPPER

The equilibrium charge state is determined by the competition between the e-loss and e-capture processes of the ions. The capture cross sections depend strongly on the ion velocity $V_p$ compared with that of the target electrons. The e-capture phenomenon is particularly highly suppressed because of poor kinematical matching when the ion velocity significantly exceeds that of the 1s electrons, $V_{1s}$, where 1s electrons are the fastest-moving target electrons. Such suppression of e-capture is expected in the case of low-Z targets or high ion velocity, because $V_{1s}$ is approximately equal to Z/137, thereby resulting in a higher equilibrium charge state for low-Z values or large ion velocities. In fact, a substantial increase in the equilibrium charge state is observed in certain experimental data on the equilibrium charge state or effective charge at intermediate energies in low-Z regions [18, 19, 20].

Table 4 summarizes the reaction conditions under which charge enhancement of the equilibrium charge state in the low-Z region is observed, along with the parameters of $V_p/V_{1s}$ (the relative projectile velocities with respect to the K-shell electrons) obtained from references [18, 19, 20]. This table also lists the parameters for the reactions for which cross-section measurements were performed in He to obtain the equilibrium charge states. These parameter values show that charge enhancement can be expected in our target reaction [U + He (gas) at 11 MeV/u]. Table 4 further lists the parameters for reactions for which equilibrium charge states were measured in $N_2$ gas; lower charge states than those obtained with carbon foils were obtained in our previous study, owing to the absence of the density effect [17, 21].

Figure 4 shows the e-loss and e-capture cross sections calculated using the binary encounter model [22] and Schlachter's formula [23] as a function of the charge state for $H_2$, He, and $N_2$. The two lines for each case intersect at the equilibrium charge state. The figure clearly shows that higher charge states are obtained in gases with Z values lower than that of $N_2$ gas. There are no data on the equilibrium charge state of uranium in a low-Z gas in this energy region mainly because of the difficulty in confining low-Z gas without using a window. For example, our gas stripper system, mentioned in the previous section, can confine only 0.015 mg/cm$^2$ of He, which is not sufficient for U ions to reach their equilibrium at 11 MeV/u, while

Table 4: Reactions for which enhancement of equilibrium charge is observed in low-Z target region. The definition of $V_p/V_{1s}$ is given in the text. The lower part of the table lists the reactions for which equilibrium charge state measurements were carried out in this study and those obtained from references of [17, 21].

| Reaction | Energy (MeV/u) | $V_p/V_{1s}$ | Ref. |
|---|---|---|---|
| Ar + $H_2$ | 1.25 | 7.1 | [18] |
| U + He | 22 | 14.9 | [19] |
| U + $N_2$ | 56 | 6.8 | [20] |
| U + He | 11 | 10.5 | |
| U + He | 14 | 11.9 | |
| U + He | 15 | 12.3 | |
| U + $N_2$ | 11 | 3.0 | |
| U + $N_2$ | 14 | 3.4 | |
| U + $N_2$ | 15 | 3.5 | |

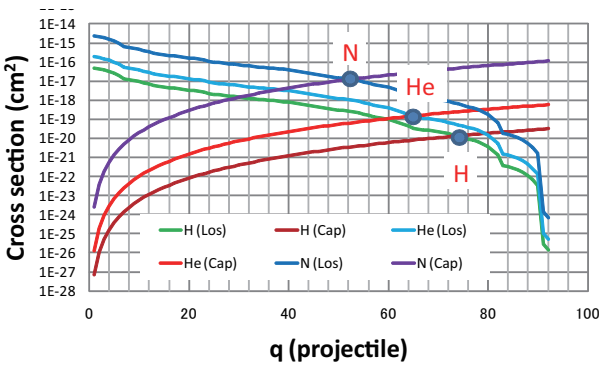


Figure 4: Simple estimation of cross sections for e-loss and e-capture in $N_2$, He, and $H_2$.

it can confine 1.3 mg/cm$^2$ of $N_2$. Hence, we measured the cross sections of the loss and capture of a 1s electron as a function of the charge state of uranium ions to extract the equilibrium charge from the intersection point of the loss and capture curves.

### *Measurements of e-Loss and e-Capture Cross Sections*

The experiment to measure the e-loss and e-capture cross sections was conducted at the RIBF using the RILAC and RRC. A schematic of the experimental setup is shown in Fig. 5. Beams of 11 MeV/u $^{238}U^{35+}$, 14 MeV/u $^{238}U^{41+}$, and 15 MeV/u $^{238}U^{41+}$ were extracted from the RRC. The incoming ions passed through a carbon foil located in front of a bending magnet, which was used to select the individual projectile charge state, $Q_i$. The thickness of the carbon foil was optimized to obtain the maximum intensity of the charge state. Each beam was directed through a windowless, differentially pumped He gas cell. After emerging from the gas cell, the beams passed through a second bending magnet into a Faraday cup (FC) at point F41 in Fig. 5.

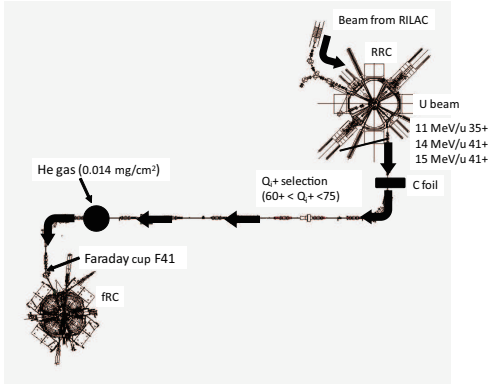


Figure 5: Schematic of experimental setup used for measurement of cross sections of e-loss and e-capture in RIBF beamlines.

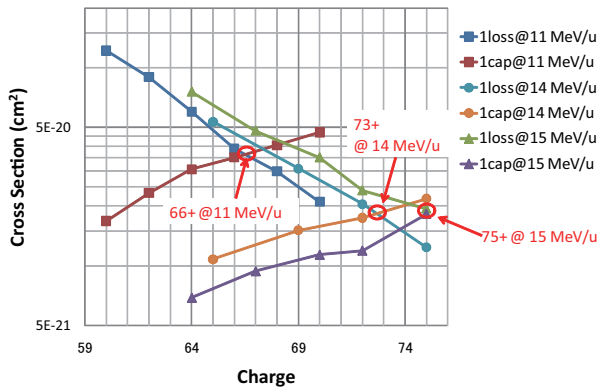


Figure 6: Measured cross sections of e-loss and e-capture as a function of the charge state of uranium ions at 11, 14, and 15 MeV/u in He gas. The cross sections were extracted assuming the thickness of the gas cell to be 13.27 μg/cm$^2$.

The FC measured the intensity of the beam current of the charge state for e-loss ($Q_i$ + 1), e-capture ($Q_i$ - 1), and no reaction ($Q_i$). The pressure of the target He gas was monitored by using a Baratron pressure transducer, and the gas flow was regulated by means of an automated control valve and a flow controller. Further details of the experimental setup can be found given in reference [17]. The cross section of e-loss, $\sigma_{loss}$, and that of e-capture, $\sigma_{capture}$, were obtained using the following equations:

$$\sigma_{loss} = \frac{1}{t}\frac{I(Q_i+1)}{\sum I(Q_m)} \quad (2)$$

$$\sigma_{capture} = \frac{1}{t}\frac{I(Q_i-1)}{\sum I(Q_m)} \quad (3)$$

where $t$ denotes the gas layer thickness and $I(Q)$ denotes the beam intensity of ion charge $Q$ at F41.

The intensity at F41 was normalized by the intensity measured by an FC located upstream of the gas cell in order to cancel the fluctuation in the beam intensity from the RRC. During the measurement, the cell pressure was maintained at a value of 0.56 kPa. At this pressure, the thickness

of the gas layer of the stripper was measured to be 13.27 ± 1.81 μg/cm$^2$ using $\alpha$-rays from $^{241}$Am.

Figure 6 shows the measured cross section as a function of the charge number of uranium ions at 11, 14, and 15 MeV/u. The absolute values of the cross sections shown in Fig. 6 have a deviation of 13.6%, although the relative values are accurate because the cross sections were extracted assuming the thickness of the gas layer to be the mean of the measurement values obtained as above. The data show that the cross section of the e-capture largely depends on the beam energy, while the e-loss cross section does not depend as much on the beam energy. Because the contribution of multiple electron transfer in He is very small [24], the intersection of the two lines gives a good approximation of the equilibrium charge state. The intersection points show charge state values of 66, 73, and 75 at 11, 14, and 15 MeV/u, respectively. Table 5 lists the equilibrium charge states in He, $N_2$, and C. The equilibrium charge state in He is obviously larger than that in $N_2$ by more than ten and is close to that in C.

Table 5: Equilibrium charge states in He, $N_2$, and C at 11, 14, and 15 MeV/u. The data for $N_2$ and C were taken from references [17, 21].

| Material | $Q_e$@11 (MeV/u) | $Q_e$@14 (MeV/u) | $Q_e$@15 (MeV/u) |
|---|---|---|---|
| He | 66 | 73 | 75 |
| $N_2$ | 56 | 61 | 62 |
| C | 72 | 76 | 77 |

### *Measurements of Charge Distributions and Energy Spread using Thick He Gas Targets*

The measurement results for e-loss and e-capture cross sections show that a low-Z gas stripper can be used to realize a higher charge state of uranium. However, the difficulty in the confinement of low-Z gases still remains due to their tendency to quickly disperse. As mentioned in the previous subsection, the existing gas stripper can confine only 0.015 mg/cm$^2$ (0.7 kPa) of He, while it can confine 1.3 mg/cm$^2$ of $N_2$. A simple estimation shows that approximately 1 mg/cm$^2$ of He or $H_2$ is necessary to achieve a higher charge state, thereby suggesting the necessity of using a new device to solve this problem. At this state, there are two options in terms of constructing a new device. The first one is the use of plasma windows, which has been described in the introduction section of this paper. We began the R&D studies on the use of plasma-window-contained strippers with A. Herschovitch because implementation of plasma window strippers requires special techniques in terms of design and operation. The plasma window was successfully ignited in October 2011 at the RIKEN site. The second option is to use large mechanical booster pumps (MBPs) to confine low-Z gas. Such MBPs are commercially available. Hence, we initiated He gas confinement at a volume of about 1 mg/cm$^2$ to measure the charge distribution and energy spread [25, 26].

Two gas strippers were prepared in order to measure the stripping performance of He and $H_2$ with cell lengths of 8 m and 0.5 m as shown in Fig. 7. The cell length was determined by the power of the differential pumping system that was available at that time. Figure 8 summarizes the measured charge evolutions in He gas as functions of the gas layer thickness. The charge is saturated around 65+, and the confinement value of 0.71 mg/cm$^2$ was selected as the optimal operational point. The fraction of 65+ is about 21% at the operational point. The energy spread after the beam was passed through a layer of 0.7 mg/cm$^2$ of He gas was measured to be preliminary around 0.4%. Although the thickness of the He gas layer is completely uniform, the energy spread is not zero due to charge exchange straggling. The energy straggling originates from the charge dependence of the energy loss and the finite width of the charge state distribution in the charge stripper. Further details are available in [27]. For the purpose of comparison, the energy spread after the beam was passed through conventionally used C foils with a thickness of 300 μg/cm$^2$ was measured to be preliminary around 0.7%.

## COMMISSIONING STATUS OF MACHINE FOR HE GAS STRIPPING

The measured data described in the previous section has enabled the conclusion that the He gas charge stripper can be used for practical operation by increasing the maximum bending power of the fRC to accept $U^{65+}$ ions though issues such as heat generation and removal and the use of a He gas recycling system require to be solved. Our choice of the new He gas stripper [28] can confine 7 kPa of He gas over a cell length of 50 cm. The total thickness of the He gas layer is 0.7 mg/cm$^2$. About 300 m$^3$/day of He gas can be circulated using 21 pumps. The stripper has a unique recycling system where the outlet of the mechanical booster pump is returned to the gas cell chamber directly. Eight order pressure reduction from 7 kPa to $10^{-5}$ Pa can be realized in order to connect the gas cell with the beam lines. Beam aperture is more than 10 mm. This system has been installed on the beam line in January, and several offline tests have been completed. Tests with U beams are in progress for a uranium beam series scheduled in the autumn of 2012. Until this time, the following issues need to be continually checked, though no major problems have been encountered thus far. Firstly, the level of impurities such as oil and water have appeared to be kept at minimum because no change in the charge distribution has been observed. Secondly, in the design phase, we were concerned with high-power beams causing ”holes” in the gas due to heat generation. However, there has been no sign of this problem from the viewpoint of the charge distribution and energy spread observed thus far. Thirdly, the He gas recycling system has been working satisfactorily, and there has been no He gas loss. In the recycling system, 98% of He

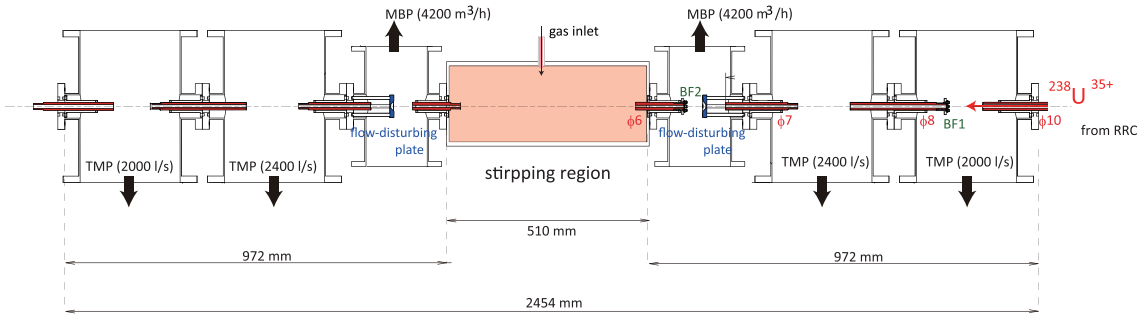


Figure 7: Schematic of 0.5-m gas cell with large differential pumping system for low-Z gas accumulation.

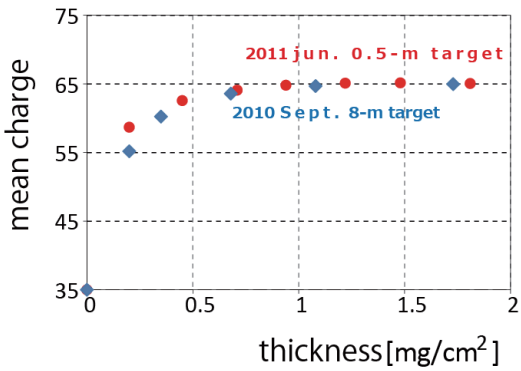


Figure 8: Measured charge evolution in He gas as a function of gas layer thickness.

gas is recycled and 2% is recovered to the He liquefier in the laboratory.

## SUMMARY

The RIBF has been successfully operated from 2007 to 2012 after the extraction of first beam. The new injector system began operation in October 2011 with objective of increasing the produced beam intensity of very heavy ions such as Xe and U ions. The stripper problem remains unresolved. However, we believe that the low-Z gas stripper is an important candidate toward addressing the issue. We carried out the following tests regarding the feasibility of using a low-Z gas stripper. First, the electron capture and loss cross sections were measured. Second, the charge evolution and energy spread were measured using a thick-layered He gas target with the large MBP system. From these two measurements, we decided to construct an actual machine for He gas stripping. We are testing the machine for the next uranium beam series in the coming autumn 2012.

## REFERENCES

[1] Y. Yano, Nucl. Instrum. Methods Phys. Res., Sect. B 261 (2007) 1009.

[2] N. Fukunishi, J. Particle Accelerator Society of Japan 4 (2007) 112.

[3] T. Nakagawa, et al., Rev. Sci. Instrum., 81 (2010) 02A320.

[4] O. Kamigaito, et al., 3rd Ann. Meeting of PASJ and 31st Linac Meeting in Japan, Sendai, (2006) 502.

[5] K. Yamada et al., IPAC'12, New Oreans, May 2012, TUOBA02.

[6] G. D. Alton and D. N. Smithe, Rev. Sci. Instrum., 65 (1994) 775

[7] T. Ohnishi, et al., J. Phys. Soc. Jpn., 79 (2010) 073201.

[8] T. Nakamura, et al., Phys. Rev. Lett., 103 (2009) 262501.

[9] P. Doornenbal, et al., Phys. Rev. Lett., 103 (2009) 032501.

[10] S. Nishimura, et al., Phys. Rev. Lett., 106 (2011) 052502.

[11] P. Ostroumov, et al., Phys. Rev. Lett. 86 (2001) 2798 .

[12] Y. Momozaki, et al., JINST 4(2009) 04005.

[13] H. Okuno, et al., Phys. Rev. ST Accel. Beams 14 (2011) 033503.

[14] A. Hershcovitch, J. Appl. Phys. 78 (1995) 5283.

[15] H. Hasebe, et al., Nucl. Instrum. Methods Phys. Res., Sect. A 613 (2010) 453.

[16] H. Ryuto, et al., Nucl. Instrum. Methods Phys. Res., Sect. A 569 (2006) 697.

[17] H. Kuboki, et al., Phys. Rev. ST Accel. Beams 13 (2010) 093501.

[18] T. Mizogawa, et al., RIKEN Accel. Prog. Rep. 22 (1988) 62.

[19] R. Bimbot, et al., Nucl. Instrum. Methods Phys. Res., Sect. B 107 (1996) 9.

[20] A. Fettouchi, et al., Nucl. Instrum. Methods Phys. Res., Sect. B 245 (2006) 32.

[21] H. Kuboki, et al., Phys. Rev. ST Accel. Beams 14 (2011) 053502.

[22] M. Gryzinski, Phys. Rev. A 138 (1965) 305; A 38 (1965) 322; A 138 (1965) 336.

[23] A. S. Schlachter, et al., Phys. Rev. A 27 (1983) 3372.

[24] H.-D. Betz, Appl. At. Coll. Phys. 4 (1983) 1.

[25] H. Imao, et al., IPAC11, San Sebastian, Sept. 2011, TUPS088.

[26] H. Imao, et al., IPAC12, New Orleans, May. 2012, TH-PPP084.

[27] H. Weick, et al., Phys. Rev. Lett. 85 (2000) 2725.

[28] H. Imao, et al., to be submitted.